JOURNAL OF MATERIALS SCIENCE 18 (1983) 3671–3678

Tempered martensite embrittlement in Fe–Ni–C steel

H. KWON, C. H. KIM
Department of Materials Science and Engineering, Korea Advanced Institute of Science and Technology, Seoul, Korea

The intergranular tempered martensite embrittlement in 6Ni–0.3C steel has been studied. For the evaluation of tempered martensite embrittlement, the impact toughness values were measured by Charpy V-notch tests. Variations in test temperature were applied to investigate its effect upon the intergranular tempered martensite embrittlement. The retained austenite was observed at the grain boundaries, as well as the lath boundaries in the as-quenched and 200° C tempered specimens. The specimen tempered at 300° C showed that the cementite platelets formed at the grain and the lath boundaries, following the decomposition of the retained austenite. The intergranular tempered martensite embrittlement associated with the formation of the grain boundary cementite was observed only when the impact test was performed below the critical test temperature (~ − 40° C). It was found that the impact toughness is controlled by the intergranular fracture below the critical test temperature, while it is controlled by the transgranular fracture (i.e. the matrix toughness) above the critical test temperature. Therefore, the grain boundary cementite platelets can produce the intergranular tempered martensite embrittlement at low test temperatures (which are below the critical test temperature) where the impact toughness is controlled by the intergranular fracture, that is, by the incorporated action of the cementite platelets and the impurities at the grain boundaries.

1. Introduction

The loss in toughness occurs when the martensitic steels are tempered in the range of 250 to 450° C although the strength continuously decreases with increasing tempering temperature. This loss in toughness has been referred to as the tempered martensite embrittlement (TME) [1–6]. The TME has been usually characterized by a trough in the plot of impact energy as a function of tempering temperature.

According to the fracture mode, the TME can be classified into two types of transgranular and intergranular TME. Transgranular TME has been generally observed in high purity steels. This embrittlement has been suggested to be attributed to the formation of interlath carbides resulting from the decomposition of the retained austenite [4, 7, 8] or carbide coarsening [6, 9]. On the other hand, the intergranular TME has been generally observed in commercial purity steels since early research. Recently, however, this embrittlement also occurred in some high purity steels [2, 10]. It has been pointed out that the incorporated action of the impurities and carbides at the grain boundaries is necessary to the intergranular TME [1–3, 10, 11]. It was found that all impurity segregation for this kind of embrittlement occurred during austenitization [12]. The microstructural changes which occur upon tempering are identical, whether the type of TME is intergranular or transgranular. However, the intergranular TME is influenced by the microstructural changes at the grain boundaries. The impact toughness is usually influenced by the test temperature and is represented by the ductile–brittle transition curve. Also, the existence of the TME is affected by the test temperatures. There were some observations about that [13, 14]. However, those results were not consistent and not definitely explained. Recently, Briant and Banerji [1] observed the intergranular TME trough in

0022–2461/83 $03.00 + .12

Ni–Cr steel only when the fracture test was performed below the ductile–brittle transition temperature of the specimen tempered near the TME temperature. In this research, the intergranular TME phenomenon has been studied in 6Ni–0.3C steel. The purposes of this study are to investigate [1] the behaviour of the retained austenite and carbides by the detailed transmission electron microscopy, and [2] the effect of test temperature on the existence of the TME.

2. Experimental procedure

About 20 kg experimental alloy ingot 100 mm × 100 mm × 250 mm was prepared by means of vacuum induction melting process. The alloy composition is listed in Table I. The ingot was then hot forged to form a rectangular bar 15 mm × 15 mm in cross-section. Three millimetre thick subsize flat tensile specimens and the standard Charpy V-notch impact specimens were made from the forged bars.

All test specimens were austenitized at 1200° C for 1 h in an argon atmosphere, and then quenched in an oil bath. Then they were immediately immersed in liquid nitrogen to complete the martensitic transformation. Austenitized specimens were tempered in a neutral salt bath at 200~600° C for 1 h and then water-quenched.

After heat treatment, the mechanical tests were done. Tensile specimens were tested on an Instron machine at a crosshead speed of 1 mm min^{-1}. From this tensile test, ultimate tensile strength, 0.2% offset yield strength and elongation data were obtained. For the impact toughness measurement, Charpy V-notch impact tests were performed. Charpy impact specimens were tested at various temperatures, to investigate the influence of test temperature.

For a detailed microstructural study, transmission electron microscopy was employed. Thin foils were prepared by utilizing the twin jet electropolishing technique, using 95% acetic acid and 5% perchloric acid electrolyte. Thin foils were examined in a Jeol electron microscope, operated at 120 kV. Bright field, selected area diffraction and dark field techniques were applied for detailed analysis.

Fracture surfaces of the impact specimens were examined in the Etec scanning electron microscope operated at 20 kV.

TABLE I Chemical composition of the experimental alloy in wt %

C	Ni	Mn	Si	S	P
0.31	5.75	< 0.01	< 0.01	0.005	0.005

3. Results

3.1. Mechanical properties

Fig. 1 shows the room temperature mechanical properties as a function of tempering temperature in 6Ni–0.3C steel. The strength levels are initially high up to 200° C tempering temperature, then rapidly decrease up to 600° C tempering temperature. This result is similar to that of 5Ni–0.25C steel studied by Huang and Thomas [15]. Thus, the alloying element nickel in Fe–Ni–C steel appears to enhance little the tempering resistance, as compared to other alloying elements, such as manganese [15], silicon [16], chromium [7], molybdenum [16, 17], tungsten [16], etc., in Fe–X–C steels. Elongation continuously increases with increases in the tempering temperature. Charpy impact energy also increases with increases in the tempering temperature. At 500° C tempering temperature, however, the increasing amount

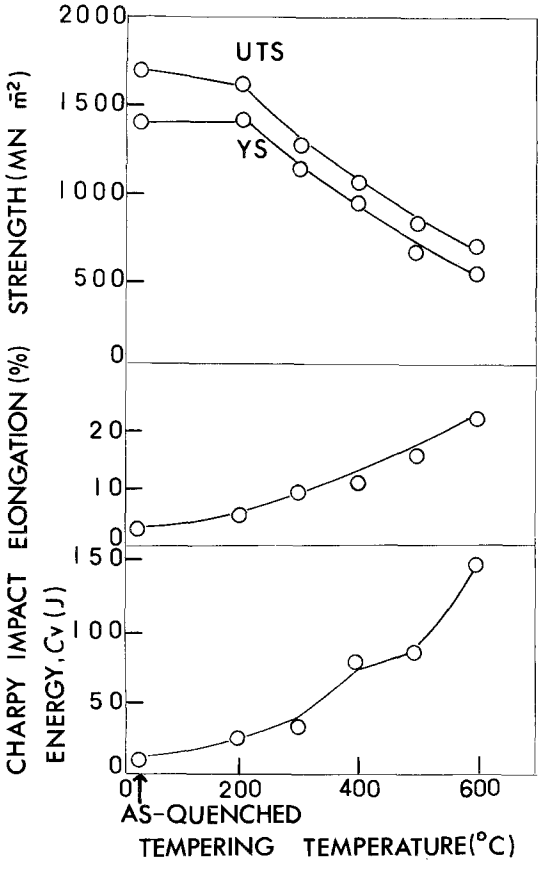

Figure 1 Room temperature mechanical properties as a function of tempering temperature.

of the impact energy is reduced. This phenomenon appears to be closely related to the temper embrittlement.

In the case of the room temperature Charpy impact test, the TME phenomenon is not observed. In order to examine the existence of the TME phenomenon, impact tests were performed at various temperatures. Fig. 2 shows the Charpy impact energy as a function of impact test temperature at 200, 300 and 400° C tempered condition. There is a critical temperature (~ −40° C) below which the TME exists. Below −40° C, the TME phenomenon explicitly exists at 300° C tempering temperature although the degree of the embrittlement is not large. Charpy impact energy as a function of the tempering temperature, is shown at various test temperatures in Fig. 3. It is clear that in Fig. 3, the TME phenomenon is present. If the ductile–brittle transition temperature is assumed as the test temperature, which corresponds to the Charpy impact energy approximately midway between the upper and lower shelf energies, the transition temperatures of the specimens tempered at 200, 300 and 400° C are approximately −20, −5 and −75° C (Fig. 2). The transition temperatures of the specimens tempered at 200 and 300° C are higher than the critical test temperature (~ −40° C). Briant and Banerji [1] observed TME phenomenon only when the fracture test was performed below the critical test temperature, which was also the transition temperature of the specimen tempered near the TME temperature. This observation also shows that TME phenomenon exists below the critical test temperature.

The upper shelf energies are approximately 30, 45 and 80 J at 200, 300 and 400° C tempered condition, respectively. As the tempering temperature decreases, the upper shelf energy level is lowered. This indicates that the upper shelf energy level varies inversely with the strength level.

3.2. Transmission electron microscopy

Transmission electron microscopy of the thin foils is essential for correlating the microstructure with the mechanical properties. In order to examine the

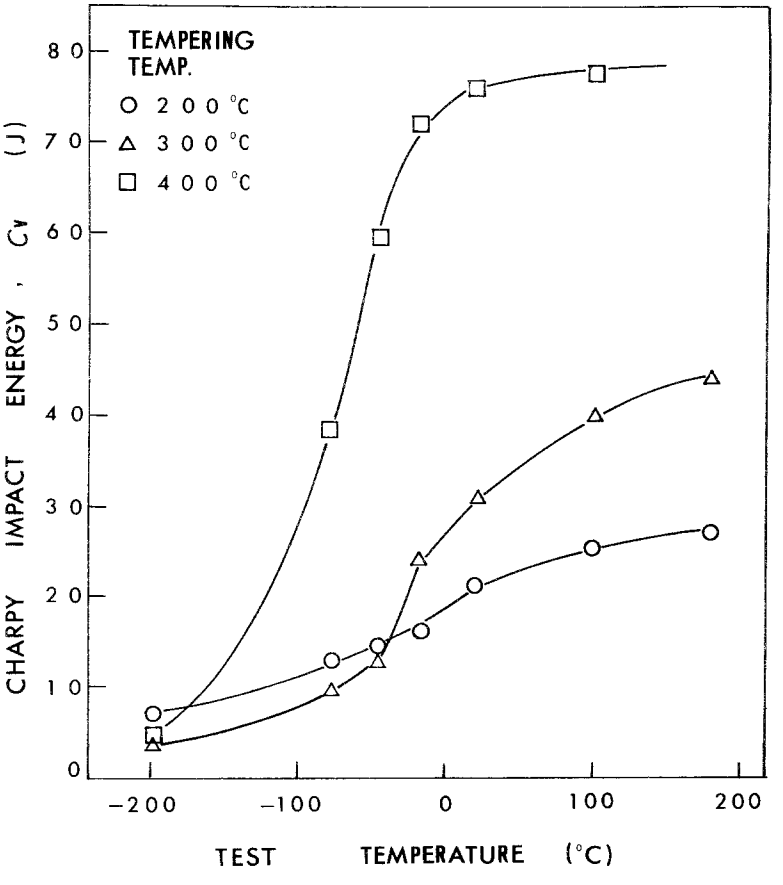

Figure 2 Charpy impact energy as a function of test temperature at 200, 300 and 400° C tempered condition, respectively.

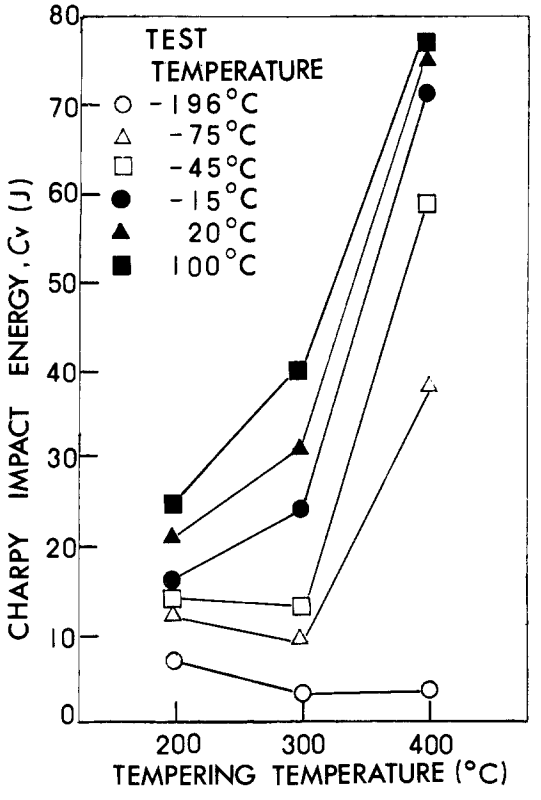

Figure 3 Charpy impact energy as a function of tempering temperature at various test temperatures.

influence of the retained austenite and carbide on the TME, the as-quenched and 300° C tempered structures have been mainly observed.

3.3.1. As-quenched structure

The structure of the as-quenched specimens consisted almost entirely of a dislocated lath type martensite. Microtwins were partially present in the laths. This martensite morphology is quite common in low alloy low and/or medium carbon steels.

Another prominent feature of the as-quenched specimen was the occurrence of autotempering. Autotempered carbides were mixtures of ϵ-carbide and cementite. Autotempering occurred because of the relatively high martensite start, M_s, temperature for 6Ni–0.3C alloy (estimated to be approximately 320° C [18]).

In the present study, the most significant point is the existence of the retained austenite. The retained austenite was first observed at the lath boundaries in Fe–Cr–C steels by McMahon and Thomas [7]. Since that time, many investigators have observed the interlath retained austenite for various alloy steels. Recently, Sastry and Wood [19] directly observed the retained austenite at the grain boundaries, as well as the lath boundaries in AISI 4340 steel. Fig. 4 shows the retained austenite at the grain boundary as well as lath boundaries in 6Ni–0.3C steel. From bright field micrograph the presence of the retained austenite at both boundaries cannot be distinguished from the boundaries alone (Fig. 4a). However, dark field micrograph clearly and unambiguously exhibits the retained austenite at both boundaries by the bright contrast (Fig. 4b).

3.2.2. Tempered structure

The structure tempered at 200° C was similar to the as-quenched structure. The retained austenite remained stable. The microstructure of the specimen tempered at 300° C, however, was markedly different from the structures observed in the as-quenched and 200° C tempered specimens. A significant change of the microstructure was observed. The retained austenite decomposed and

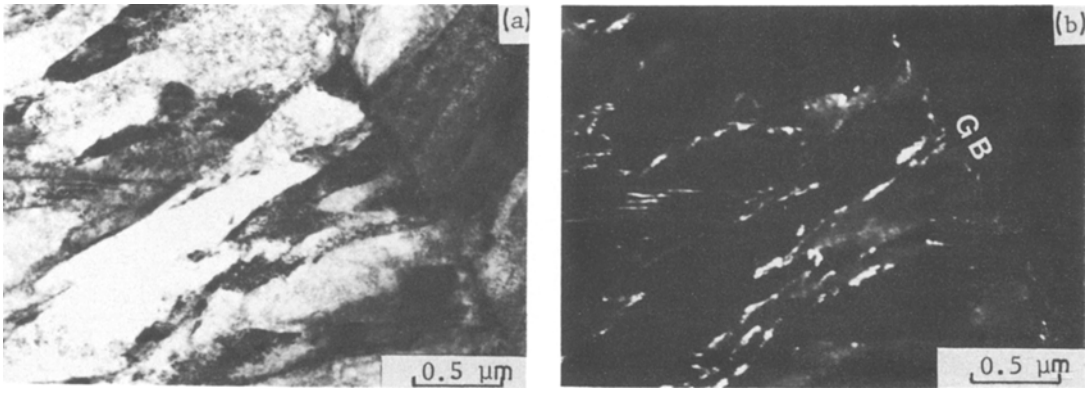

Figure 4 Retained austenite in the as-quenched condition, (a) BF and (b) DF micrographs showing the austenite at the grain boundary as well as the lath boundaries in bright contrast.

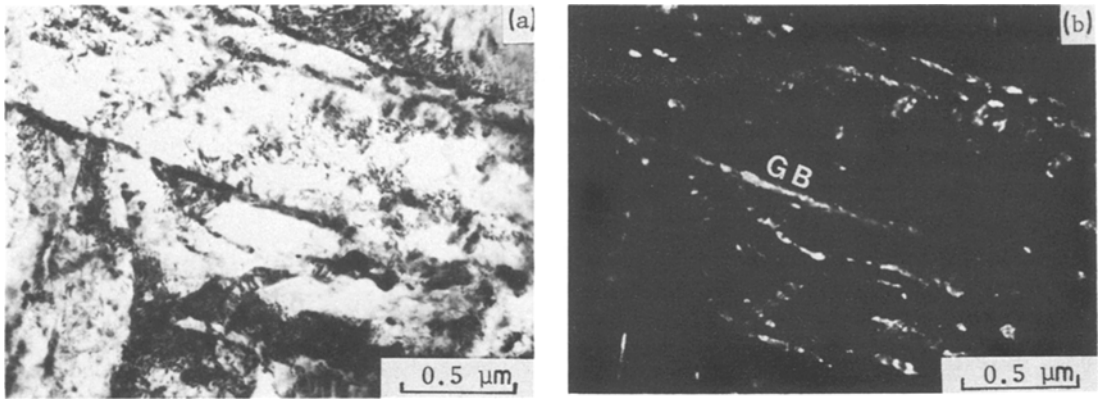

Figure 5 Cementite formation resulting from the decomposition of the retained austenite at 300° C tempered condition. (a) BF and (b) DF micrographs showing the cementite at the grain boundary as well as the lath boundaries in bright contrast.

the cementite was formed at the lath and the grain boundaries. Fig. 5 shows the cementite formed at the lath and the grain boundaries. From the bright field micrograph, cementite at both boundaries cannot be identified (Fig. 5a). However, the dark field micrograph clearly and unambiguously shows the cementite at both boundaries by the bright contrast (Fig. 5b). The cementite formation at both boundaries is extensive. The cementite is coarse and platelike. The cementite platelets at the grain boundaries may play a significant role for the intergranular TME phenomenon, as will be discussed later.

3.3. Fractography

A fractographic observation must be performed to link the TME phenomenon with the microstructure. For the impact specimens tempered at 200 and 300° C, the fracture surfaces have been observed by the scanning electron microscope. Fig. 6 shows the fracture surfaces of the specimens fractured at −75° C, where the TME exists. The fracture mode of the specimen tempered at 200° C was a mixture of the intergranular and transgranular fracture. The fracture surface exhibited cleavage and some dimples. The exposed grain boundaries of the fracture surface

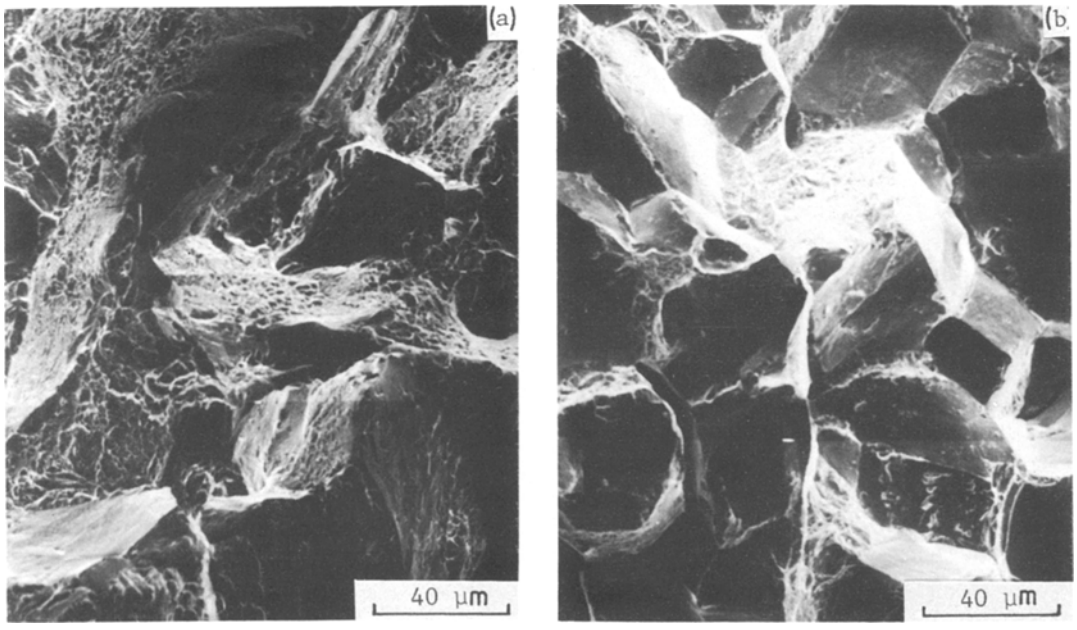

Figure 6 Fractographs of the specimens fractured at −75° C, (a) 200° C tempered condition and (b) 300° C tempered condition.

have a relatively rough nature typical of the specimen lacking the grain boundary carbides. On the other hand, the specimen tempered at 300° C mostly shows the brittle intergranular fracture surface. The smooth nature of the brittle intergranular fracture is typical of the specimen with grain boundary carbides. From this result, it is expected that the grain boundary carbides are formed at 300° C tempering temperature. The fracture surfaces of the specimens fractured at room temperature, where the TME does not exist are shown in Fig. 7. The ductile fracture area increased in both 200 and 300° C tempered specimens. The specimen tempered at 300° C still shows the exposed grain boundaries, which are smoother than those of the specimen tempered at 200° C. This result indicates that the presence of the grain boundary carbides influences the fracture mode although the grain boundary carbides cannot cause the TME phenomenon to occur at room temperature. However, the intergranular fracture area decreased and the transgranular fracture area increased relatively with increases in the test temperature. The transgranular fracture area mostly shows dimples by the microvoid coalescence, compared to the cleavage nature of the intergranular fracture area. Thus, the room temperature impact toughness appears to be dependent upon the energy forming the transgranular fracture area.

4. Discussion

Tempered martensite embrittlement can be classified into two types by the fracture mode; transgranular and intergranular TME. Transgranular TME has been suggested to be associated with the formation of the interlath carbides resulting from the decomposition of retained austenite [4, 7, 8], or with the carbide coarsening [6, 9]. On the other hand, it has been proposed that the intergranular TME is attributed to the combination of impurity segregation and carbide precipitation at the grain boundaries [1–3, 10, 11]. It is known that impurity segregation occurs during austenitization in this kind of embrittlement [12]. Thus, after quenching, the grain boundaries will be enriched in some impurities (phosphorus and/or sulphur) and the concentration of impurities will not change before tempering at relatively high temperatures ($>\sim 400°$ C). Impurity segregation at the grain boundaries was observed even in some high purity steels (S, P < 0.005 wt %) [2, 10]. Also, these steels exhibited the intergranular TME. From the observation of the intergranular fracture it is believed that the impurity segregation also occurs in the present steel (Fig. 6). The grain boundary carbides are formed during tempering near TME temperature. The TME phenomenon is associated with the formation of the carbides at the grain boundaries. Materkowski and Krauss [3] investi-

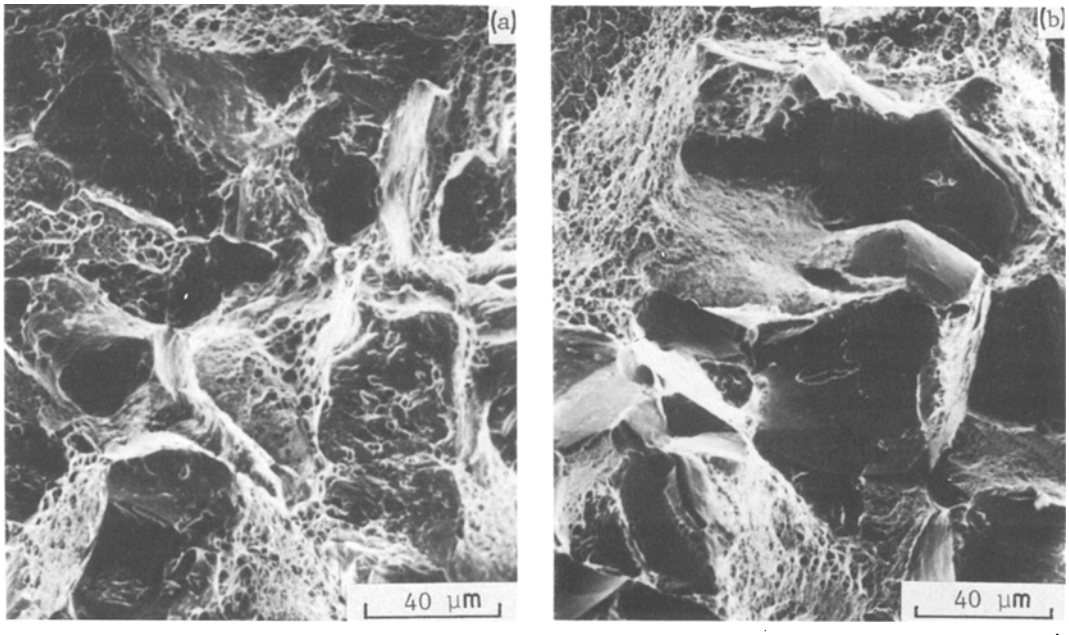

Figure 7 Fractographs showing the surfaces mixed of the intergranular and dimple nature of the specimens fractured at room temperature, (a) 200° C tempered condition and (b) 300° C tempered condition.

gated the intergranular and the transgranular TME with the impact toughness troughs in the same temperature range of 250 to 400° C for high phosphorus (0.03 wt %) and low phosphorus (0.003 wt %) AISI 4340 steels. From this observation it is believed that the mechanism of the carbide formation at both the lath and grain boundaries will be identical. Recently, Sastry and Wood [19] directly observed the grain boundary retained austenite in AISI 4340 steel. Thus the grain boundary carbides as well as the lath boundary carbides appear to form, following the decomposition of the retained austenite.

In the present study the retained austenite at both the lath and the grain boundaries has been observed in 6Ni–0.3C steel (Fig. 4). At 300° C tempering temperature, the retained austenite decomposed and the cementite platelets were formed at the lath and the grain boundaries as shown in Fig. 5. The cementite platelets were coarse. For this steel, it is likely that carbide coarsening would also occur for 1 h tempering period at 300° C. Upon 300° C tempering, initially the formation of the cementite platelets following the decomposition of the retained austenite occurs and later they coarsen. The decomposition of the retained austenite initially determines the cementite morphology which is important for the TME phenomenon. This cementite morphology is plate-like along the lath and the grain boundaries. Later, carbide coarsening occurs and it is accompanied by matrix softening. Matrix softening will increase the impact toughness. It is uncertain whether the impact toughness increases or decreases at the initial stage of carbide coarsening before rapid matrix softening. However, if the impact toughness decreases or remains at a low level at this stage, it would be due to maintaining the cementite morphology during carbide coarsening rather than carbide coarsening alone, on condition that matrix softening would hardly increase the impact toughness. Hence, for the TME phenomenon, the basic cause of the loss in toughness is associated with the formation of the cementite following the decomposition of the retained austenite. The intergranular TME is connected with the formation of the cementite at the impurity weakened grain boundaries, following the decomposition of the retained austenite. The grain boundary cementite platelets can act as the effective slip barriers to dislocation. The dislocation pile-ups at the grain boundary cementite platelets can initiate intergranular cracks at the impurity-weakened carbide–matrix interfaces. Thus, the grain boundaries with the cementite platelets can be easily separated than those without the cementite platelets. The cementite platelets at the impurity weakened grain boundaries will lower the fracture energy. This leads to the intergranular TME.

However, TME is not observed at all test temperatures (Figs. 2 and 3). There is a critical test temperature ($\sim -40°$ C) below which the TME trough is observed. Above the critical test temperature, no TME trough is observed. Briant and Banerji [2] observed the intergranular TME for Ni–Cr steel only when the fracture test was performed below the transition temperature of the specimen tempered near the TME temperature. From these results it is clear that for the observation of an intergranular TME trough the fracture test has to be performed below the critical test temperature. Below the critical test temperature ($\sim -40°$ C), the specimen tempered at 300° C mostly shows the intergranular fracture surface which is smooth and clean (Fig. 6b). This indicates that the grain boundary cementite platelets play a role as brittle crack initiaters. Thus the cementite platelets resulting from the decomposition of the retained austenite at the impurity weakened grain boundaries enhanced the degree of the intergranular fracture and lowers the intergranular fracture energy. The impact toughness of the specimen tempered at 300° C will be controlled by the intergranular fracture. However, the degree of the intergranular fracture decreases with increases in the test temperature. Thus the contribution of the intergranular fracture to the impact toughness decreases and that of the transgranular fracture to the impact toughness increases with increases in the test temperature. Above the critical test temperature ($\sim -40°$ C), the contribution of transgranular fracture to the impact toughness becomes relatively prevalent. Transgranular fracture energy increases as the matrix toughness increases with increases in the tempering temperature. However, the intergranular fracture surface of the specimen tempered at 300° C is still more clean and smooth, compared to that of the specimen tempered at 200° C. The grain boundary cementite platelets can act as the crack initiaters even above the critical test temperature.

However, the effect of the grain boundary weakening due to impurity segregation may not be sufficient for the grain boundaries to act as the

easy fracture path above the critical test temperature. Thus the impact toughness may be controlled by the transgranular fracture (i.e. matrix toughness). The impact toughness of the specimen tempered at 300° C is higher than that of the specimen tempered at 200° C. The intergranular TME does not exist at higher test temperatures where the impact toughness is controlled by the transgranular fracture.

Therefore the intergranular TME exists only when the grain boundary cementite platelets can act as the crack initiaters and these cracks can propagate easily along the grain boundaries, which are already weakened by the impurity segregation. This condition can be satisfied below the critical test temperature. Below the critical test temperature, the fracture mode is mainly intergranular and the impact toughness is controlled by the intergranular fracture.

5. Conclusions

1. The retained austenite exists at the grain boundaries as well as the lath boundaries in the as-quenched and 200° C tempered structure.

2. A significant change was observed at 300° C tempering temperature. The retained austenite decomposed and the cementite platelets formed at the grain and the lath boundaries.

3. TME was observed at 300° C tempering temperature only when the impact test was performed below the critical test temperature ($\sim -40°$ C).

4. The intergranular TME was associated with the formation of the cementite platelets following the decomposition of retained austenite at the impurity weakened grain boundaries.

5. The intergranular TME may exist only if the impact toughness can be controlled by the intergranular fracture. This condition can be satisfied below the critical test temperature ($\sim -40°$ C) where both the cementite platelets and the impurities at the grain boundaries can make the grain boundaries the easy fracture path.

6. Above the critical test temperature, the impact toughness will be controlled by the transgranular fracture (i.e. the matrix toughness). Although the intergranular cracks can be initiated by the grain boundary cementite platelets, the effect of the grain boundary weakening caused by the impurity segregation is not sufficient for the intergranular cracks to propagate easily along the grain boundaries. Thus, the intergranular TME cannot exist above the critical test temperature.

References

1. C. L. BRIANT and S. K. BANERJI, *Met. Trans. A* **10A** (1979) 1729.
2. *Idem, ibid.* **10A** (1979) 1151.
3. J. P. MATERKOWSKI and G. KRAUSS, *ibid.* **10A** (1979) 1643.
4. G. THOMAS, *ibid.* 9A (1978) 439.
5. R. M. HORN and R. O. RITCHIE, *ibid.* 9A (1978) 1039.
6. H. K. D. H. BHADESHIA and D. V. EDMOND, *Met. Sci.* **13** (1979) 325.
7. J. McMAHON and G. THOMAS, Proceedings of the Third International Conference on Strength of Metals and Alloys, Vol. 1 (Institute of Metals, London, 1973) p. 180.
8. B. V. N. RAO and G. THOMAS, *Met. Trans. A* **11A** (1980) 441.
9. J. E. KING, R. F. SMITH and J. F. KNOTT, Fracture 1977-ICF4, Vol. 2, edited by D. M. R. Taplin (University of Waterloo Press, Waterloo, 1977) p. 279.
10. S. K. BANERJI, C. J. McMAHON Jr and H. C. FENG, *Met. Trans. A* 9A (1978) 237.
11. C. L. BRIANT and S. K. BANERJI, *Int. Met. Rev.* **23** (1978) 164.
12. T. OGURA, C. J. McMAHON, Jr., H. C. FENG and V. VITEK, *Acta Metall.* **26** (1978) 1317.
13. R. L. RICKETT and J. M. HODGE, *Proc. ASTM* **21** (1951) 931.
14. L. J. KLINGLER, W. J. BARNETT, R. P. FROHMBERG and A. R. TROIANO, *Trans. ASM* **46** (1954) 1557.
15. D. H. HUANG and G. THOMAS, *Met. Trans.* **2** (1971) 1587.
16. H. KWON, PhD thesis, Korea Advanced Institute of Science and Technology, Seoul, Korea (1983).
17. R. A. CLARK and G. THOMAS, *Met. Trans. A* **6A** (1975) 969.
18. W. STEVEN and A. HAYNES, *J. Iron Steel Inst.* **183** (1956) 349.
19. C. N. SASTRY and W. E. WOOD, *Mater. Sci. Eng.* **45** (1980) 277.

Received 18 October 1982
and accepted 29 March 1983